Latin American Journal of Aquatic Research

E-ISSN: 0718-560X

lajar@pucv.cl

Pontificia Universidad Católica de Valparaíso

Chile

Montero, Paulina; Daneri, Giovanni; Tapia, Fabián; Iriarte, Jose Luis; Crawford, David

Diatom blooms and primary production in a channel ecosystem of central Patagonia

Latin American Journal of Aquatic Research, vol. 45, núm. 5, noviembre, 2017, pp. 999-1016

Pontificia Universidad Católica de Valparaíso

Valparaíso, Chile

Lat. Am. J. Aquat. Res., 45(5): 999-1016, 2017
DOI: 10.3856/vol45-issue5-fulltext-16


*Research Article*

# Diatom blooms and primary production in a channel ecosystem of central Patagonia

**Paulina Montero[1,2], Giovanni Daneri[1,2], Fabián Tapia[2,3,4], Jose Luis Iriarte[2,5,6] & David Crawford[1]**
[1]Centro de Investigación en Ecosistemas de la Patagonia (CIEP), Coyhaique, Chile
[2]COPAS Sur-Austral, Universidad de Concepción, Concepción, Chile
[3]Departamento de Oceanografia, Universidad de Concepción, Concepción, Chile
[4]INCAR, Universidad de Concepción, Concepción, Chile
[5]Instituto de Acuicultura, Universidad Austral de Chile, Puerto Montt, Chile
[6]Fondap-IDEAL, Universidad Austral de Chile, Valdivia, Chile
Corresponding author: Paulina Montero (pmontero@ciep.cl)

**ABSTRACT.** Here we report on the seasonal productivity cycle at a fixed station in the Puyuhuapi Channel (44ºS, 73ºW), Chilean Patagonia. The analysis of *in situ* water column data and longer-term records of satellite-derived surface ocean color (Chl-*a*) highlighted two contrasting seasons. A more productive period occurred between August and April, where depth-integrated gross primary production (GPP) estimates ranged from 0.1 to 2.9 g C $m^{-2}$ $d^{-1}$, and a shorter, less-productive season lasted from May to July with GPP ranging from 0.03 to 0.3 g C $m^{-2}$ $d^{-1}$. Diatoms of the genera *Pseudo-nitzschia*, *Skeletonema* and *Chaetoceros* dominated the phytoplankton, and showed a pronounced seasonality greatly influenced by prevailing environmental conditions. Warmer waters were associated with high concentrations of *Pseudo-nitzschia* spp., while high abundances of *Skeletonema* spp. and *Chaetoceros* spp. were associated with fresher silicate-rich waters. A marked *Skeletonema* spp. bloom characterized the onset of the productive season in August 2008, and with some exceptions, the highest levels of GPP (1.5 to 2.9 g C $m^{-2}$ $d^{-1}$) were measured when *Skeletonema* dominated the phytoplankton community. Reduced production (low GPP) was observed during periods of increased discharge from the Cisnes River, whereas the "spring" diatom bloom (or late winter bloom in Puyuhuapi Channel) observed during August 2008 coincided with a ~50% drop in the freshwater discharge. We therefore suggest that periods of intensive freshwater Input, that increase the silicic acid concentrations in the upper layers, provide ideal growing conditions for diatoms as the freshwater flow subsequently recedes. Principal component analysis (PCA) suggests that a decrease in salinity, increase in silicic acid concentration, and growth of *Skeletonema* spp. and *Chaetoceros* spp., are probably key factors in the annual cycle of GPP in Puyuhuapi Channel.

**Keywords:** primary production, diatom blooms, channels ecosystem, Chilean fjords.

## INTRODUCTION

Chilean Patagonia encompasses one of the most extensive fjord regions in the world (Iriarte *et al.*, 2014), with oceanographic conditions that can sustain unique ecosystems. Among the highly productive ecosystems found in the SE Pacific, the coastal upwelling system that spans the coast of central and northern Chile has been the focus of most research conducted over the past decades, although it is restricted to a relatively narrow coastal band (<50 km, Montecino *et al.*, 2006). Patagonian fjords, on the other hand, comprises *ca.* 240,000 $km^2$ of highly productive coastal waters (Iriarte *et al.*, 2014), and constitute eco-systems that have an enormous potential in terms of total productivity, transfer of food to higher trophic levels, and vertical export of carbon. Improving our understanding of primary productivity cycles and composition of phytoplankton communities in these waters is therefore of fundamental importance.

The productivity cycle within a number of Patagonian channels and fjords (41-51ºS) has been typically described in terms of two contrasting seasons: a productive season characterized by a marked spring diatom bloom followed by pulsed productivity events dominated by a sequence of different phytoplankton species, and then a non-productive season that predominantly features small phytoplankton cells (Iriarte

Corresponding editor: Sergio Palma

*et al.*, 2007; Iriarte & González, 2008; Czypionka *et al.*, 2011; Montero *et al.*, 2011; Paredes & Montecinos, 2011). Despite considerable recent research, uncertainty remains regarding the factors that modulate the seasonal phase change within Chilean fjords system, from non-productive in late autumn-winter to highly productive in late winter-autumn. It is not clear whether similar factors control productivity cycles throughout of these channels and fjords, or whether the main environmental controls on these productivity cycles may vary across the region.

The onset of the productive season in Patagonia has been associated with mesoscale changes in the direction and intensity of meridional winds. Montero *et al.* (2011) reported that the onset of the productive season in the Reloncaví Fjord (41°S, 72°W) coincided with a late winter relaxation of prevailing poleward winds. This seasonal shift in predominant winds and improved light conditions has been shown to influence the productivity of fjord and channel ecosystems (Iriarte & González, 2008; Montero *et al.*, 2011). More locally, hydrodynamic patterns within a given fjord are strongly modulated by freshwater discharges, which can either intensify or weaken an estuarine type of circulation, and may modulate the occurrence and spatial extent of phytoplankton blooms (Goebel *et al.*, 2005; González *et al.*, 2013; Iriarte *et al.*, 2014; Jacob *et al.*, 2014). Freshwater inputs appear to stabilize the water column and increase the concentration of silicic acid in the upper layers, favouring the occurrence of diatom dominated phytoplankton blooms.

Diatoms are capable of fast growth and are well adapted to form large blooms (Wetz & Wheeler, 2007). They account for *ca*. 40% of the total oceanic primary production, making them a significant component of marine food webs (Sarthou *et al.*, 2005; Amin *et al.*, 2012), and key players in global biogeochemical cycles (Ferland *et al.*, 2011). Certain species are able to completely dominate a phytoplankton community (Legrand *et al.*, 2003). In Chilean fjords ecosystems, diatoms are known to represent a significant component of the overall phytoplankton biomass (Iriarte *et al.*, 2001; Cassis *et al.*, 2002; Alves-de-Souza *et al.*, 2008; Iriarte & González, 2008). In addition to efficiently transferring energy to higher trophic levels, diatoms make a significant contribution to the downward transfer of organic carbon (Iriarte *et al.*, 2007; González *et al.*, 2010; Montero *et al.*, 2011; Iriarte *et al.* 2013). Diatoms occur in highest abundance during the Patagonian fjord spring bloom, and are generally dominated by *Skeletonema* spp. and associated with high levels of primary production (Iriarte *et al.*, 2007; Montero *et al.*, 2011). Despite the significant contribution that diatoms make to overall fjord productivity, important questions remain unanswered: for example, which are the main factors that trigger diatom blooms in specific fjords and channels, and which are the key species in terms of significance to annual productivity.

In this study, we characterized the seasonal productivity cycle at a fixed station in the Puyuhuapi Channel (44ºS, 73ºW). The hydrography of the northern Puyuhuapi Channel is characterized by an estuarine type of circulation with a vertical two layer structure comprising a highly variable 5-10 m freshwater layer, and a more uniform and saltier subpycnocline layer (Schneider *et al.*, 2014 and references therein). The deeper saline water originates from Sub-Antarctic Surface Water characteristic of open ocean environments in these latitudes (Chaigneau & Pizarro, 2005). The freshwater upper layer is supplied by the Cisnes River, several smaller rivers, and rain runoff, and it is a permanent feature of the Puyuhuapi Channel, although the degree of mixing with deeper saline water is seasonally variable (Schneider *et al.*, 2014). Based on recent studies in other fjord ecosystems in the region, we hypothesized that the seasonal pattern of productivity in the Puyuhuapi area may be strongly influenced by freshwater input with a consequential series of blooms dominated by diatom species.

Gross primary production (GPP) and community respiration (CR) were measured in order to assess the trophic status of the water column in the study area on a seasonal basis. Finally, we analyzed the relationships between the main environmental variables (phytoplankton species composition, dissolved inorganic nutrients, temperature, salinity) and their potential association with seasonal changes in GPP of the study area.

## MATERIALS AND METHODS

### Study area and sampling strategy

The study area consisted of a fixed station in the Puyuhuapi Channel (44°42.6'S, 72°44.4'W), located at an average depth of 230 m and *ca.* 5 km NW of the Cisnes River mouth (Fig. 1). The channel runs in a N-NE direction and connects directly to the open sea via the Moraleda Channel at its mouth, and through the Jacaf Channel near the head (Schneider *et al.*, 2014; Fig. 1). The Puyuhuapi Channel receives freshwater discharge from the Ventisqueros (north and south), Pascua and Cisnes rivers, plus additional inputs from numerous creeks and rainfall (Calvete & Sobarzo, 2011). The freshwater input drives an estuarine type of circulation, with a thin layer of freshwater flowing from the continent, on top of a thicker layer of oceanic Sub-

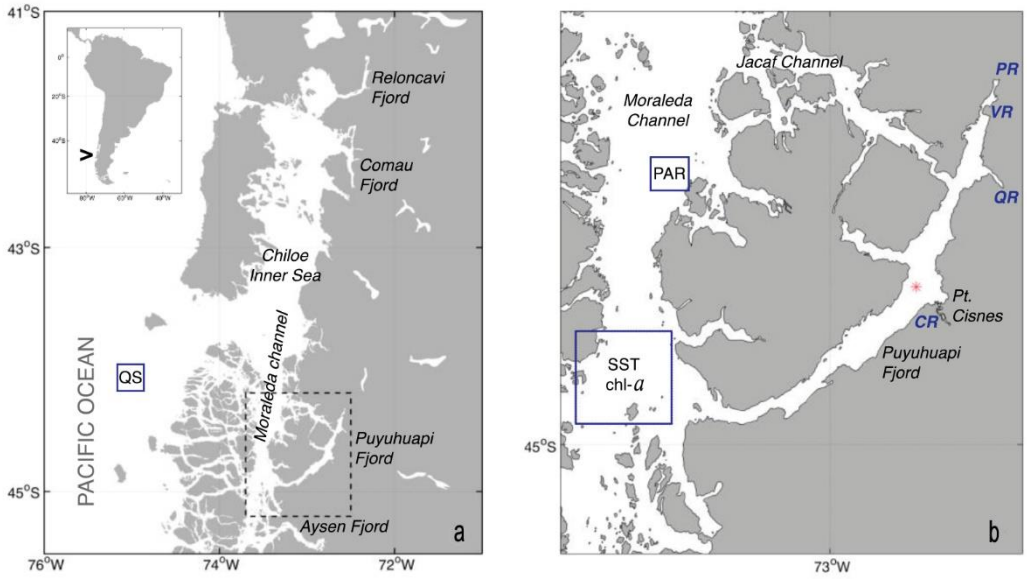


**Figure 1.** Location of the study area in Chilean Patagonia (A: dashed box enlarged in b) and position of the time series station in the Puyuhuapi Channel (B: asterisk). Solid squares in a and b indicate the points/areas for which satellite data on wind stress (QS), photosynthetically active radiations (PAR), Sea Surface Temperature (SST) and surface chlorophyll-*a* concentration (Chl-*a*) were obtained (see methods for details). Position of main rivers are indicated in (b) and correspond to the Cisnes (CR), Queulat (QR), Ventisquero (VR), and Pascua (PR) rivers.

Antarctic Waters (Silva *et al.*, 2009; Schneider *et al.*, 2014). Freshwater coming from the continent is loaded with silicic acid while Sub-Antarctic Waters (SAAW) is enriched with nitrate and orthophosphate (Silva, 2008). The Puyuhuapi Channel is an area of intensive salmon farming, and consequently receives large inputs of particulate and dissolved organic matter from both autochthonous (phytoplankton productivity) and allochthonnnous sources (freshwater input and aquaculture).

Sampling at the Puyuhuapi station was conducted approximately at monthly intervals between January and November 2008. Additionally, in summer (January 2008 and March 2009), autumn (April 2009), winter (May and July 2008) and spring (October 2008 and September 2009) intensive sampling campaigns (over periods of 3-7 consecutive days) were conducted.

### Variability of atmospheric and sea-surface conditions

Satellite-derived data, dating from 2003 through late 2009, were used to characterize variability in atmospheric forcing and sea-surface conditions in an area close to the study site (Fig. 1). Data on wind stress were collected over a 25×25 km area from daily QuikSCAT level-3 images. This area represented a pixel centered on 44°7.5'S, 75°7.5'W, and located *ca*. 170 km NW of the channel's mouth. Good data were available from 96.6% of the 2471 records available for this pixel in 2003-2009. A time series of photosynthetically available radiation (PAR) for the same period was produced from 8-d composites of SeaWifs images (level 3), with a 9 km resolution. Data were acquired for a pixel centered at 44°30'S, 73°25'W, in the Moraleda Channel and *ca*. 50 km NW of the channel's mouth. Out of the 295 PAR images available for this pixel in 2003-2009, 98% contained good data. Finally, data on sea surface temperature (SST) and surface chlorophyll-*a* concentration (Chl-*a*) were acquired from 8 d composites of MODIS-Aqua images (level 3) with a 4 km spatial resolution. Weekly values of surface Chl-*a* were obtained by averaging data collected over a 5×7 pixel area (*i.e.*, 20×35 km) located near the mouth of the fjord, encompassing the latitudes 44°47.5'-44°57.7'S and longitudes 73°37.5'-73°22.5'W (see Fig. 1). Out of the 273 Chl-*a* and 314 SST images available for this area in 2003-2009, 78% and 94% contained good data. Any gaps within these four records of satellite-derived data were filled using linear interpolation.

### Hydrography, nutrients and phytoplankton composition

Profiles of temperature, salinity and dissolved oxygen were gathered during each sampling day using a CTDO profiler (Ocean Seven 304, IDRONAUT, Italy). Water samples for analyses of inorganic nutrients and phyto-

plankton abundance were collected from three discrete depths (2, 10, and 20 m) using a 30-L Niskin bottle (General Oceanic, Inc.).

Water samples for nutrient analyses were filtered through GF/F filters and frozen at -20°C prior to spectrophotometric analysis in the laboratory. Concentrations of nitrate, orthophosphate, and silicic acid were determined according to methods given in Strickland & Parsons (1968). Samples for phyto-plankton cell counts were stored in 250 mL clear plastic bottles, preserved in a 1% Lugol iodine solution (alkaline). From each sample, a 10 mL sub-sample was placed in a sedimentation chamber and allowed to settle for 12 h (Utermöhl, 1958) prior to identification at 40 × and 100 × under an inverted microscope (Carl Zeiss, Axio Observer A.1). Estimates of phytoplankton (in the size range 2-200 μm) abundance at the three discrete depths were integrated down to 20 m, using a trapezoidal method.

**Total and size-fractionated primary production and chlorophyll-*a* (Chl-*a*)**

During each field campaign between January 2008 and September 2009, *in situ* experiments were conducted to measure gross primary production (GPP) and community respiration (CR). A total of 37 experiments were conducted and water incubations were performed on samples obtained from the same sampling depths indicated above (2, 10 and 20 m). GPP and CR rates were estimated from changes in dissolved oxygen concentrations observed during *in situ* incubation of light and dark bottles (Strickland, 1960). Water from the Niskin bottles was transferred into 125 mL (nominal volume) borosilicate bottles (gravimetrically calibrated) using a silicone tube. Five time-zero bottles, five light bottles, and five dark bottles were used for each incubation depth. Water samples were collected at dawn and were incubated during the whole light period (incubating time was 10.0 ± 1.3 h in the productive period (September-April) and 7.0 ± 0.7 h during the non-productive season (May-August). Time-zero bottles were fixed at the beginning of each experiment, whereas the light and dark incubation bottles were attached to a surface-tethered mooring system. The samples were incubated at the depth from which they were collected. Dissolved oxygen concentrations were determined according to the Winkler method (Strickland & Parsons, 1968), using an automatic Metrohom burette (Dosimat plus 865) and by visual end-point detection. Problems with the power supply in this isolated location prevented us from using a photometric end point detector. Daily GPP and CR rates were calculated as follows: GPP = (mean [$O_2$] light bottles - mean [$O_2$] dark bottles); CR = (mean [$O_2$] time zero bottles - mean [$O_2$] dark bottles) / (hours of incubation) ×24. GPP and CR values were converted from oxygen to carbon units using a conservative photosynthetic quotient (PQ) of 1.25 (Williams & Robertson, 1991) and a respiratory quotient (RQ) of 1. Discrete-depth estimates of GPP and CR rates were integrated down to 20 m using a trapezoidal method. The 20 m depth layer approximately corresponded to the 1% light depth measured during the productive season (21.7 ± 8.2; calculated using a Secchi disc as in Poole & Atkins, 1929). For total Chl-*a* determinations, three 100 mL water samples were filtered from each of the three sampling depths through MFS (Micro-filtration Systems) glass-fiber filters with 0.7 μm nominal pore size. Following filtration, samples were immediately frozen (-20ºC) until later analysis; pigments were extracted with 90% v/v acetone and then measured using a Turner Design TD-700 fluorometer according to standard procedures (Parsons *et al.*, 1984).

In order to provide additional information on the relative contribution of various size fractions to overall PP, primary production (PP) was estimated using the $^{14}C$ method (Steeman-Nielsen, 1952). Water samples were collected using Niskin bottles at 2, 10 and 20 m and placed in 100 mL polycarbonate bottles (two clear + one dark) to which were added 40 μCi labelled sodium bicarbonate ($NaH^{14}CO_3$). Bottles were placed in a natural light incubator for 4 h during the time of day with highest irradiance (approximately between 11 AM and 3 PM). Temperature was regulated in the incubator using a flow through of surface seawater. For the subsurface samples, light intensity was attenuated using a screen to approximately the level found at the depth where water was collected. Samples were manipulated under subdued light conditions during pre- and post-incubation periods. At the end of the incubations, samples were filtered for size fractionation as described below. Filters were then placed in 20 mL plastic scintillation vials and stored at -15ºC prior to analysis. Within one month, filters were dried in a fume-chamber for 48 h and the excess inorganic carbon was removed with HCl fumes for 24 h; 10 mL Ecolite liquid scintillation cocktail was added to vials which were then processed using a Beckman Liquid Scintillation Counter.

Size fractionation was performed on Chl-*a* and PP (post-incubation) samples using the following three size classes to separate the phytoplankton assemblage: microphytoplankton (>20 μm), nanophytoplankton (2-20 μm), and picophytoplankton (<2 μm). This size fractionation was performed on samples in three sequential steps: (1) for the nanophytoplankton fraction (2-20 μm), seawater (100 mL) was pre-filtered using 20 μm Nitex mesh and collected on a 2 μm Nuclepore

filter; (2) for the picoplankton fraction (0.2-2.0 µm), the filtrate from the 2 µm Nuclepore filter in step (1) was filtered again using a 0.7 µm MFS glass-fiber filter; (3) for the whole phytoplankton community, seawater (100 mL) was filtered through a 0.7 µm MFS glass-fiber filter. The microphytoplankton fraction was obtained by subtracting the estimated PP and Chl-*a* in steps (1) and (2) from the estimates in step (3). Depth-integrated values of PP and Chl-*a* were calculated down to 20 m, using trapezoidal integration. This size fractionation of Chl-*a* and PP was only conducted during the intensive sampling campaigns.

### Statistical analyses

Cross-correlation analyses was conducted to test for associations between satellite-derived time series of meridional wind stress, surface PAR, SST, and surface Chl-*a* concentration. To assemble a set of data vectors that were amenable to these analyses, a weekly series of cumulative meridional wind stress was produced based on the initial and final dates of the composite Chl-*a* images. Climatologies of PAR, SST, and Chl-*a* series were used to calculate anomalies prior to the computation of lagged correlation coefficients. The significance levels for each of these analyses were computed according to the method outlined in Sciremammano (1979, see equations 7 and 16b). The 2 m sampling depth was used to represent upper mixed layer conditions because the pycnocline was located at approximately 6 m depth. The non-parametric Kruskal-Wallis test (H) was used to examine and test for significance of seasonal differences in GPP and CR. Clustering analysis was used to investigate temporal variation in phytoplankton community structure. A similarity matrix among samples was calculated using the Bray & Curtis method (1957), and a dendrogram constructed based on group average linkage. Given that several of our environmental measurements were non-independent (*e.g.*, salinity, temperature, inorganic nutrients, phytoplankton community, Chl-*a*), a principal component analysis (PCA) was conducted to combine these original variables into statistically independent environmental predictors for GPP. The data used in this analysis for temperature, salinity, and inorganic nutrients were depth-averages calculated over the upper 20 m, whereas phytoplankton community and Chl-*a* data corresponded to depth-integrated values calculated down to 20 m. A Spearman correlation analysis ($r_s$) was then conducted to assess the degree of association between these principal components and log-transformed GPP values.

## RESULTS

### Variability of atmospheric and sea-surface conditions

The 7-year time series of QuikSCAT data on meridional wind stress showed an alternation of periods with equatorward and poleward winds, each persisting for several days, with a scale of correlation of *ca*. 5 d, and no apparent annual pattern (Fig. 2a). This lack of a clear pattern of seasonal variability in wind forcing, and its high inter-annual variability, became more apparent in the climatology computed for wind stress (Fig. 2e). In contrast, surface PAR and SST time series showed a strong annual cycle (Figs. 2b-2c), which was also reflected by the low inter-annual variability (*i.e.* small error bars) shown in the climatology (Figs. 2f-2g).

Average daily PAR varied between *ca.* <10 E $m^{-2}$ $d^{-1}$ in winter and >40 E $m^{-2}$ $d^{-1}$ in summer, and average surface temperature between ca. 8 to 9°C in winter and >14°C in summer. Surface chlorophyll concentrations, on the other hand, showed high intra- and inter-annual variability with peaks of over 30 mg $m^{-3}$ (Fig. 2d).

The climatology shows the existence of two distinct seasons: a low- chlorophyll (presumably less productive) period that spans the autumn and winter months (April-August) with concentrations averaging <5 mg $m^{-3}$, and a productive season in spring and summer (September-March) with average concentrations typically in the range 10 to 20 mg $m^{-3}$, typified by high seasonal variability (Fig. 2h). Phytoplankton biomass tended to increase rapidly in spring (September-October), decay in summer (December-January), and increase again in late summer (February-March, see Fig. 2h).

Surface PAR and SST were highly correlated at lag = 0 ($r = 0.64$, $P < 0.001$) and reached maximum correlation ($r = 0.77$, $P < 0.001$) at ~40 day lag, with increases in PAR preceding increases of SST. This high correlation combined with the lack of a clear annual signal in wind stress variability, suggest that the strong seasonality in SST near the Puyuhuapi Channel is mostly driven by changes in solar radiation. Weak but significant zero-lag correlations were found for surface Chl-*a* and cumulative meridional wind stress ($r = 0.35$, $P < 0.01$), PAR anomalies ($r = 0.30$, $P < 0.01$) and SST anomalies ($r = 0.23$, $P < 0.01$).

### *In situ* hydrographic and nutrient measurements

In general, the water column was characterized by a two-layer structure largely determined by vertical salinity changes (Fig. 3a), with the halocline usually being found above 10 m depth. Salinity profiles showed a surface layer (2 m) of low-salinity water (<20), particularly during productive periods (2008 and 2009) (Fig. 3a), while surface values >20 (21 to 25) were recorded during the non-productive period (2008). Below this layer and between 10 and 100 m depth, salinity fluctuated between 30 and 33 (Fig. 3a). Surface temperature decreased from >18°C in January 2008 to <7°C in August 2008 and from >15ºC in March 2009

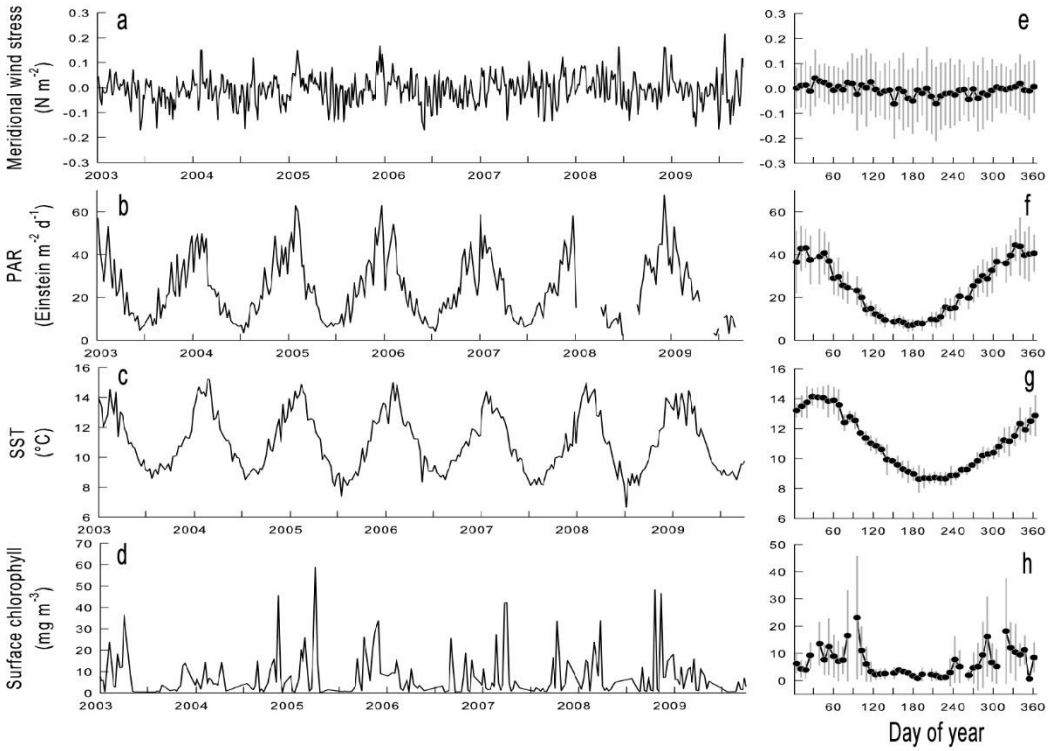


**Figure 2**. Satellite-derived time series (A-D) and climatologies (E-H) of meridional wind stress (A, E), surface PAR, *i.e.*, Photosynthetically Available Radiation (B, F), Sea Surface Temperature (C, G), and surface chlorophyll-*a* concentration (D, H). Wind stress data were obtained from daily QuikSCAT level-3 images with ~25 km spatial resolution, PAR data were produced from 8-d composites of SeaWifs images with 9 km resolution, whereas SST and Chl-*a* were extracted from 8-d composites of MODIS-Aqua images with 4 km resolution. See methods for more details. Symbols and error bars in E-H correspond to the mean ±1 SD.

to <9ºC in September 2009; these are similar ranges to those shown for the time series station (Figs. 2c, 2g) although maximum temperatures at the time series station were a little lower because of the greater influence of oceanic water. Thermal stratification decreased during May/June 2008 and September 2009, while winter cooling lead to a thermal inversion in July and August 2008 (Fig. 3b). Surface oxygen concentration increased from 3 to 4 mL $O_2$ $L^{-1}$ during warm periods to 6 to 8 mL $O_2$ $L^{-1}$ during cold periods. Maximum values (>8 mL $O_2$ $L^{-1}$) were recorded in October 2008 (Fig. 3c). Low dissolved oxygen concentrations (<3 mL $O_2$ $L^{-1}$) were observed during January and February 2008 below 20 and 30 m of depth, respectively. Then in April and September 2009 low oxygen values were also recorded below 50 m depth. For the rest of the study period, values were >3 mL $O_2$ $L^{-1}$ into the depth layer.

Low surface concentrations of nitrate (<3 µM) were observed within the top 10 m during the productive periods in 2008 and 2009, while maximum concentrations of >10 µM were recorded in the non-productive months (Fig. 4a). Low orthophosphate concentrations (<1 µM) were observed within the top 10 m throughout most of the sampling, except in July 2008 and September 2009, where values ranged between 1 and 3.5 µM, with highest values occurring in September 2009 at 2 and 10 m. Orthophosphate concentrations were typically >1 µM at 30 m depth. Orthophosphate concentrations did not show marked seasonal differences (Fig. 4b). Silicic acid concentrations showed moderate surface concentrations (4 to 30 µM) during 2008 and very high surface values (100 to 132 µM) in 2009. Generally, concentrations were higher in surface waters than at 20 m depth (Fig. 4c). The increase in surface silicic acid coincided with the inputs of low-salinity water in the same period (shown in Fig. 3a).

## Primary production and community respiration

The highest rates of GPP derived from $O_2$ incubations (0.3 to 47.9 mmol $O_2$ $m^{-3}$ $d^{-1}$) were recorded at 2 m depth, whereas the lowest values (0.1 to 11.8 mmol $O_2$ $m^{-3}$ $d^{-1}$) were observed at 20 m depth (Fig. 5a). CR rates showed the highest values at 20 m depth (0.3 to 27.9 mmol $O_2$ $m^{-3}$ $d^{-1}$), with the lowest observed at 10 m

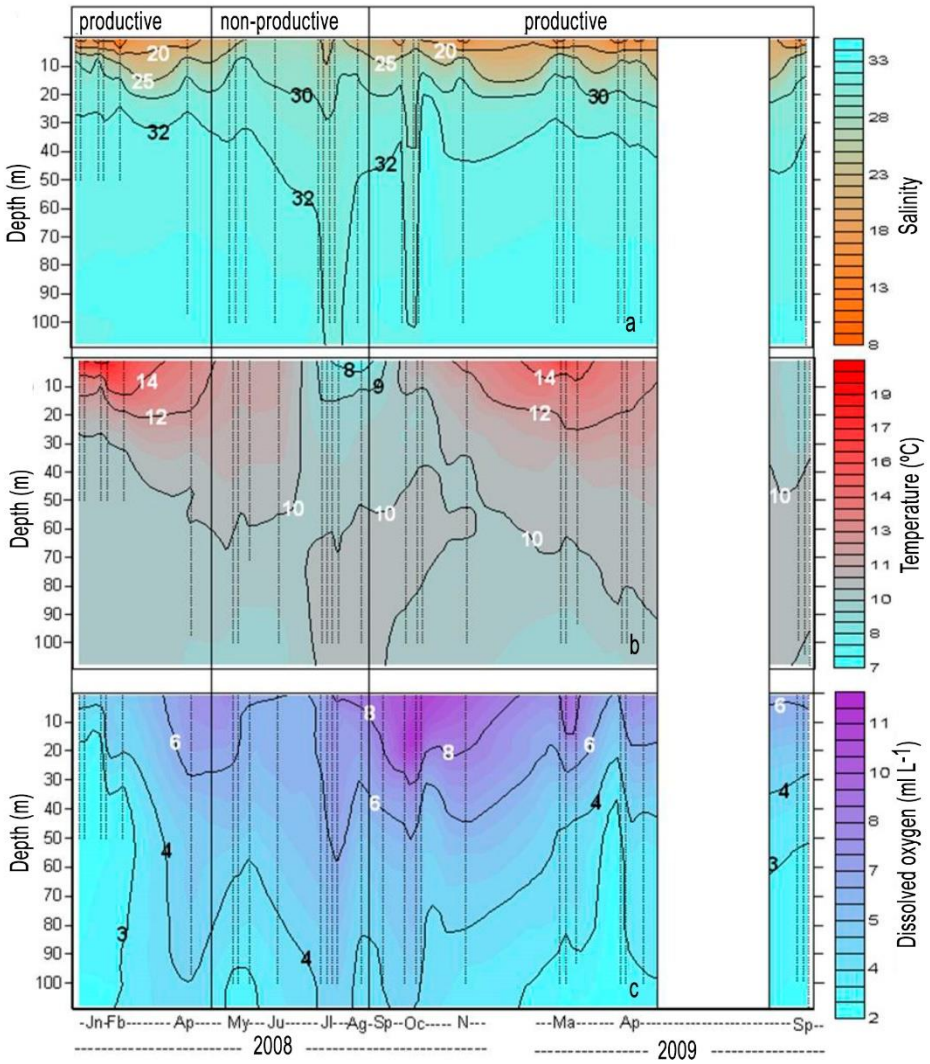


**Figure 3.** Temporal variability of hydrographic profiles at the Puyuhuapi Channel station: a) salinity, b) temperature (ºC), and c) dissolved oxygen (ml $L^{-1}$). Sampling times and depth range are indicated by dotted vertical lines.

depth (0.1 to 17.3 mmol $O_2$ $m^{-3}$ $d^{-1}$). GPP/CR ratio, used as an index for the trophic status of the system, ranged from 0.01 to 17, with most experiments indicating a heterotrophic metabolism (GPP/CR < 1) (Fig. 5b).

Depth-integrated GPP showed significant differences between the productive and non-productive seasons ($H = 8$, $P < 0.05$, $n = 37$). Integrated GPP (down to 20 m) ranged from 0.03 to 2.9 g C $m^{-2}$ $d^{-1}$ over the annual cycle (Fig. 5c) with highest rates recorded during late winter and spring in August (2.9 g C $m^{-2}$ $d^{-1}$) and November 2008 (2.4 g C $m^{-2}$ $d^{-1}$), and low values (0.03 to 0.3 g C $m^{-2}$ $d^{-1}$) observed from May to July 2008. Depth-integrated CR rates also showed significant seasonal differences ($H = 6$, $P < 0.05$, $n = 37$), with values ranging from 0.04 to 3.4 g C $m^{-2}$ $d^{-1}$ over an annual cycle (Fig. 5c). Maximum values were recorded in November 2008 (3.2 g C $m^{-2}$ $d^{-1}$) and April 2009 (3.4 g C $m^{-2}$ $d^{-1}$), while low rates (0.04 to 1 g C $m^{-2}$ $d^{-1}$) were consistently observed in winter 2008.

The highest estimates of contribution of microphytoplankton (>20 µm) to total $^{14}C$ fixation (mean: 49%; range: 15 to 83%; n = 15) were recorded during the productive season, whereas picophytoplankton (<2 µm) showed maximum contributions (mean: 60%; range: 38 to 81%) during the non-productive season (Table 1). The nanophytoplankton size class (2-20 µm) did not show significant seasonal variations in contribution to total $^{14}C$ fixation. Depth-integrated GPP and PP values were positively correlated ($r_s = 0.68$, $P < 0.05$, $n = 23$; Fig. 6), although the slope of the regression indicates that $^{14}C$ derived PP tends to be higher than GPP.

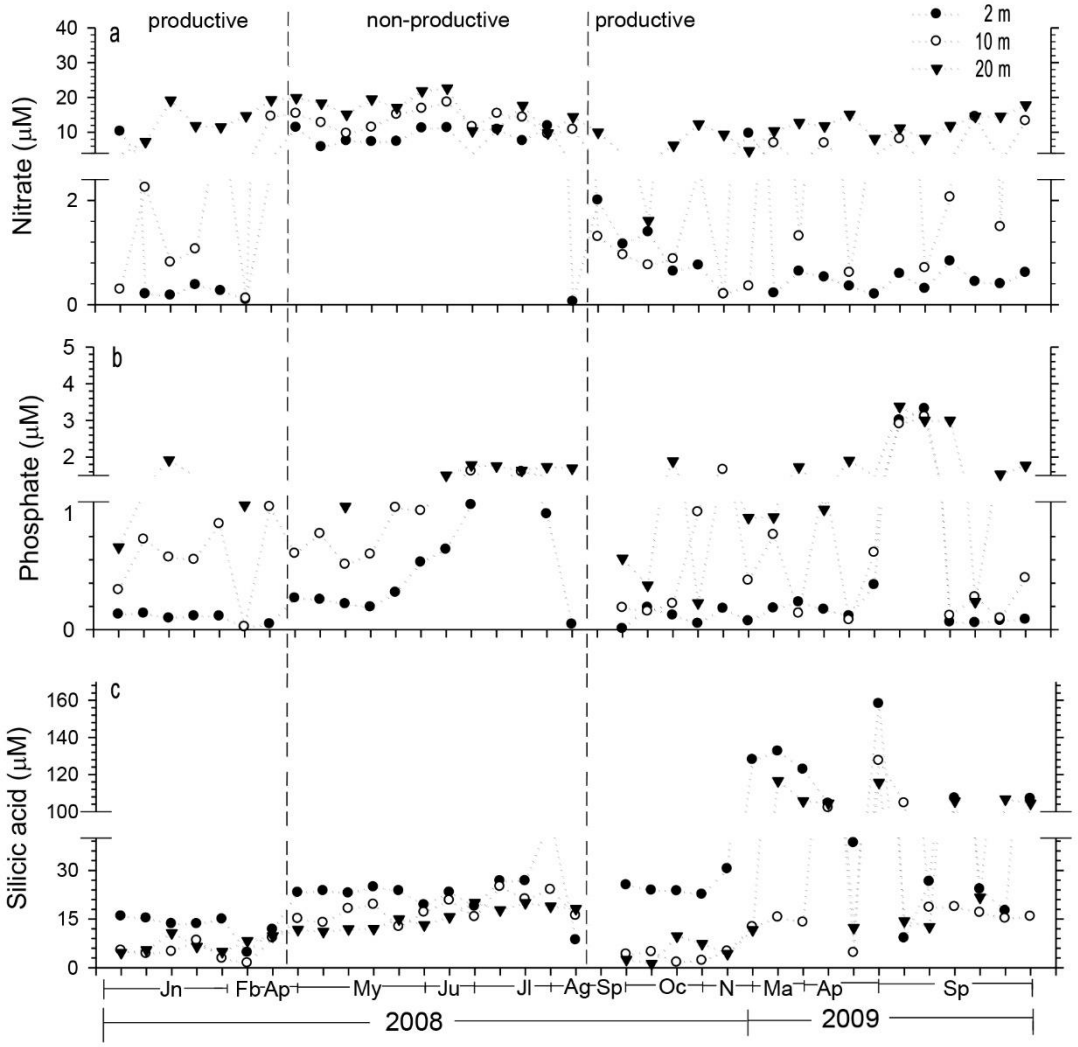


**Figure 4.** Temporal variability of dissolved inorganic nutrients at three depths at the Puyuhuapi station: a) nitrate, b) phosphate, and c) silicic acid. Sampling times and depths are indicated by dots.

### Chlorophyll-*a* and phytoplankton community

The maximum depth-integrated phytoplankton biomass (166.2 mg Chl-*a* $m^{-2}$) was observed in late winter (August 2008), and coincided with the highest GPP measurements (2.9 g C $m^{-2}$ $d^{-1}$); other than this maximum value, biomass ranged from 2.8 to 75.7 mg Chl-*a* $m^{-2}$ in the productive season and 1.8 to 15.8 mg Chl-*a* $m^{-2}$ in the non-productive season (Fig. 7).

Estimates of Chl-*a* partitioned into three size classes (<2 µm, 2-20 µm, >20 µm) revealed the dominance of picophytoplankton (<2 µm) during the non-productive season (May and July) throughout the entire water column. During the productive season, picophytoplankton was dominant only in January 2008 and September 2009 at 20 m depth (Table 1). Chlorophyll in the nanophytoplankton size class (between 2-20 µm) did not show significant variations over the annual cycle. Strong seasonal variability was observed for microphytoplankton (>20 µm), which showed a high relative contribution to total Chl-*a* during the productive season at 2 and 10 m depths; in contrast, low relative contributions were recorded during the non-productive season (Table 1).

Diatoms were the dominant group within the community, averaging 92% of microscope-examined phytoplankton abundance, followed by dinoflagellates (7%) and ciliates (1%).

Of the total recorded diatoms, five genera were the most abundant during the study period: *Skeletonema* (*S. costatum* and *S. pseudocostatum*), *Pseudo-nitzschia* (*Pseudo-nitzschia* spp. group *seriata* and *Pseudo-nitzschia* spp. group *delicatissima*), *Chaetoceros* (*Ch. decipiens*, *Ch. convolutus*, *Ch. didymus*, *Ch. radicans*, *Ch. curvisetus*, *Ch. debilis*, *Ch. similis*, *Ch. mitra* and

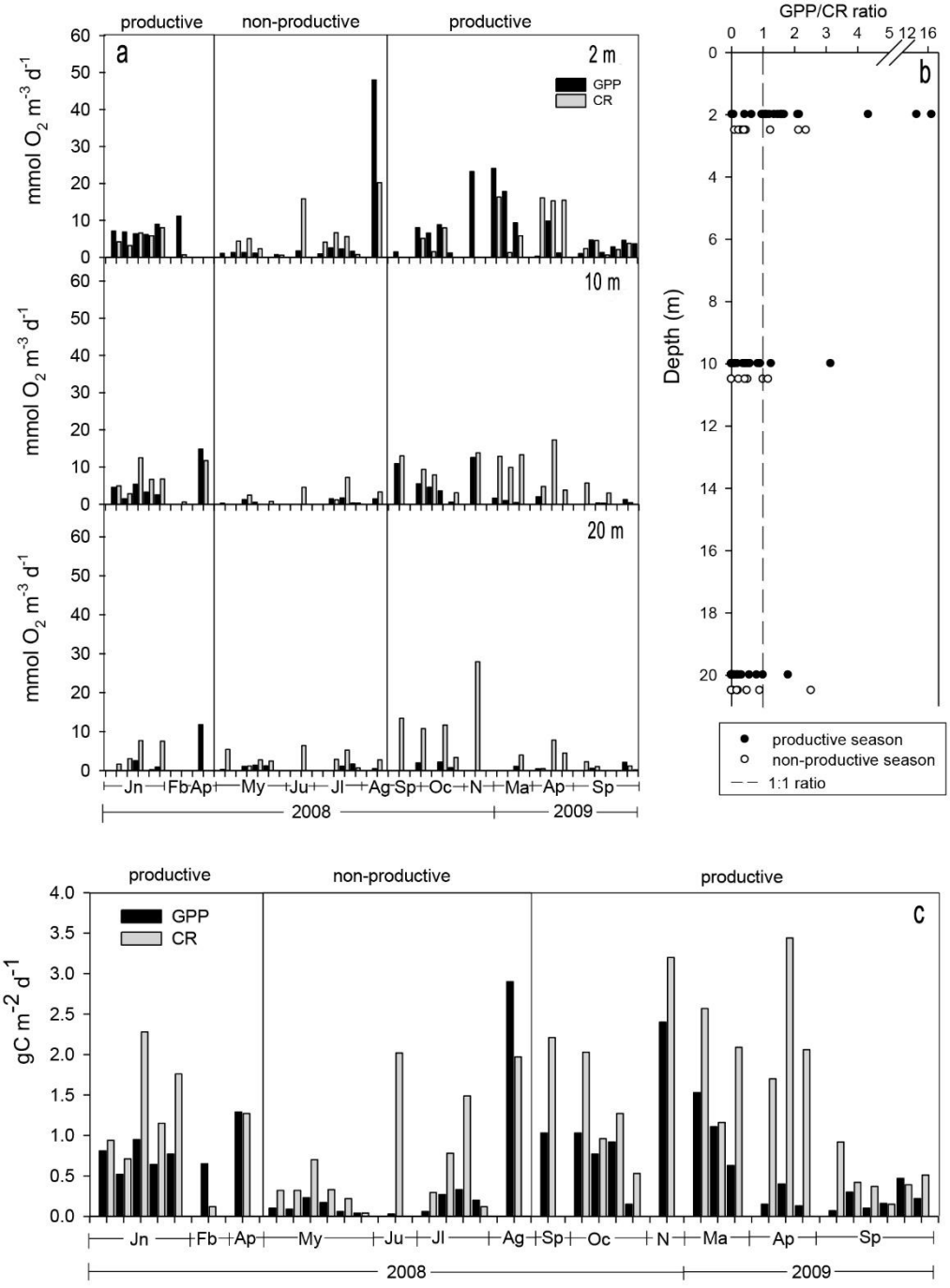


**Figure 5.** Vertical variability of gross primary production (GPP) and community respiration (CR) rates at the Puyuhuapi station. a) Seasonal changes in GPP and CR at three depths, b) vertical profile of GPP/CR ratios for all samples, and c) depth-integrated GPP and CR using dissolved oxygen changes converted to carbon units.

*Chaetoceros* sp.), *Thalassiosira* (*T. anguste-lineata*, *T. excentrica* and *Thalassiosira* sp.) and *Leptocylindrus* (*L. minimus* and *L. danicus*) (Fig. 8a).

*Skeletonema* spp., *Pseudo-nitzschia* spp. and *Chaetoceros* spp. were dominant and in more than one sampling contributed with values >50% of the total phytoplankton abundance, unlike *Thalassiosira* spp. and *Leptocylindrus* spp. that never reached or exceeded this percentage (Fig. 8a). The highest abundances of *Skeletonema* spp. ($113\times10^9$ cells $m^{-2}$), *Pseudo-nitzschia* spp. ($163\times10^9$ cells $m^{-2}$) and *Chaetoceros* spp. ($63\times10^9$ cells $m^{-2}$) were recorded in August, February and October

**Table 1.** Contribution of microphytoplankton (>20 µm), nanophyoplankton (2-20 µm), and picophytoplankton (<2 µm) to total carbon ($^{14}C$) fixation rates. Total chlorophyll-*a* concentration at three depths during the intensive sampling, at the Puyuhuapi station.

| Depth | Date | Contribution to total carbon fixation (%) | | | Contribution to total chlorophyll-*a* (%) | | |
|---|---|---|---|---|---|---|---|
| | | < 2 µm | 2-20 µm | >20 µm | < 2 µm | 2-20 µm | >20 µm |
| 2 m | January 08 | 25 | 44 | 31 | 22 | 31 | 47 |
| | May 08 | 38 | 29 | 33 | 39 | 32 | 29 |
| | July 08 | 52 | 35 | 13 | 40 | 18 | 42 |
| | October 08 | 11 | 20 | 69 | 26 | 13 | 61 |
| | March 09 | 5 | 14 | 81 | 17 | 13 | 70 |
| | April 09 | 8 | 11 | 81 | 44 | 9 | 47 |
| | September 09 | 7 | 21 | 72 | 21 | 19 | 60 |
| 10 m | January 08 | 39 | 22 | 39 | 32 | 19 | 50 |
| | May 08 | 65 | 27 | 8 | 45 | 31 | 24 |
| | July 08 | 57 | 32 | 11 | 44 | 23 | 33 |
| | October 08 | 11 | 16 | 73 | 19 | 17 | 64 |
| | March 09 | 22 | 26 | 52 | 15 | 11 | 74 |
| | April 09 | 7 | 10 | 83 | 39 | 22 | 39 |
| | September 09 | 10 | 48 | 41 | 30 | 14 | 56 |
| 20 m | January 08 | 51 | 30 | 20 | 45 | 25 | 30 |
| | May 08 | 79 | 11 | 10 | 50 | 38 | 12 |
| | July 08 | 67 | 22 | 11 | 44 | 23 | 33 |
| | October 08 | 41 | 36 | 23 | 25 | 11 | 64 |
| | March 09 | 60 | 24 | 15 | 21 | 24 | 55 |
| | April 09 | 40 | 22 | 38 | 41 | 48 | 11 |
| | September 09 | 9 | 70 | 20 | 39 | 24 | 37 |

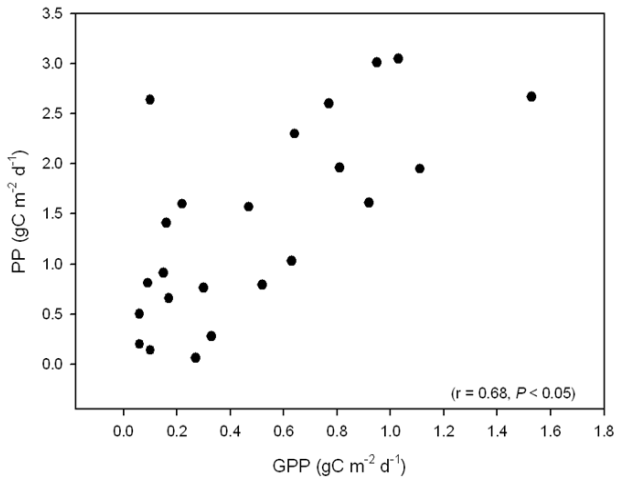


**Figure 6.** Correlation between gross primary production (GPP), using the oxygen technique, and primary production (PP) rates, estimated using $^{14}C$ technique at the Puyuhuapi station, during the intensive sampling campaigns.

2008, respectively, while low abundance values (5 to $25\times10^9$ cells $m^{-2}$) were observed in April (*Skeletonema* spp. and *Pseudo-nitzschia* spp.) and September 2009 (*Chaetoceros* spp.). *Thalassiosira* spp. were present throughout the study period, showing the highest ($64\times10^9$ cells $m^{-2}$) and lowest ($<2\times10^9$ cells $m^{-2}$) abundances in January 2008 and September 2009, respectively. *Leptocylindrus* spp. were only recorded in September 2009 with abundances between 5 and $10\times10^9$ cells $m^{-2}$ (Fig. 8a).

Diatoms that contributed <10% of the total phytoplankton abundance per sample such as *Actinoptychus vulgaris*, *Corethron hystrix*, *Coscinodiscus* sp., *Detonula pumila*, *Ditylum brightwellii*, *Eucampia zodiacus*, *Lauderia annulata*, *Guinardia delicatula*, *Melosira nummuloides*, *Rhizosolenia setigera*, *Rhizosolenia pungens*, *Stephanopyxis turris*, *Licmophora* sp., *Asterionella glacialis*, *Grammatophora marina*, *Thalasionema nitzschoides*, *Cylindrotheca closterium*, *Pleurosigma* sp. and *Nitzschia longissima* were grouped into the "other diatoms" group. This group showed its highest abundances (5 to $11\times10^9$ cells $m^{-2}$) in September 2009, however, it was in May 2008 when they dominated the phytoplankton community with abundances between 2 and $7\times10^9$ cells $m^{-2}$. The lowest abundances ($<1\times10^9$ cells $m^{-2}$) were observed in January and February 2008.

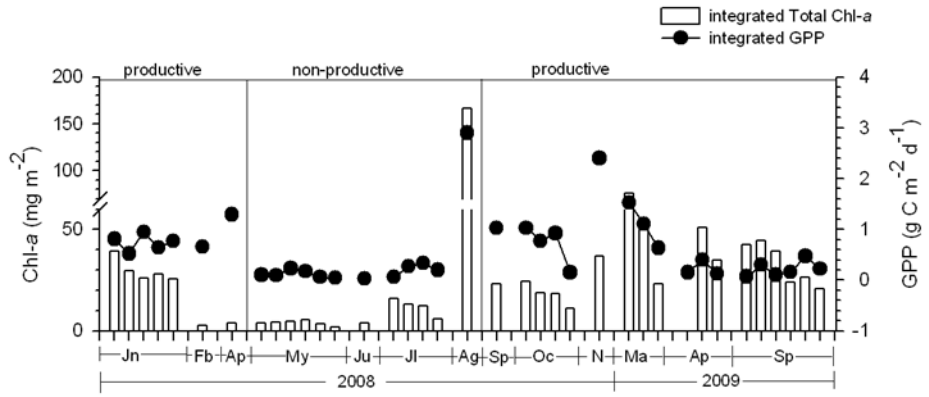


**Figure 7.** Temporal variability of depth-integrated (0-20 m) total chlorophyll-*a* and GPP at the Puyuhuapi station.

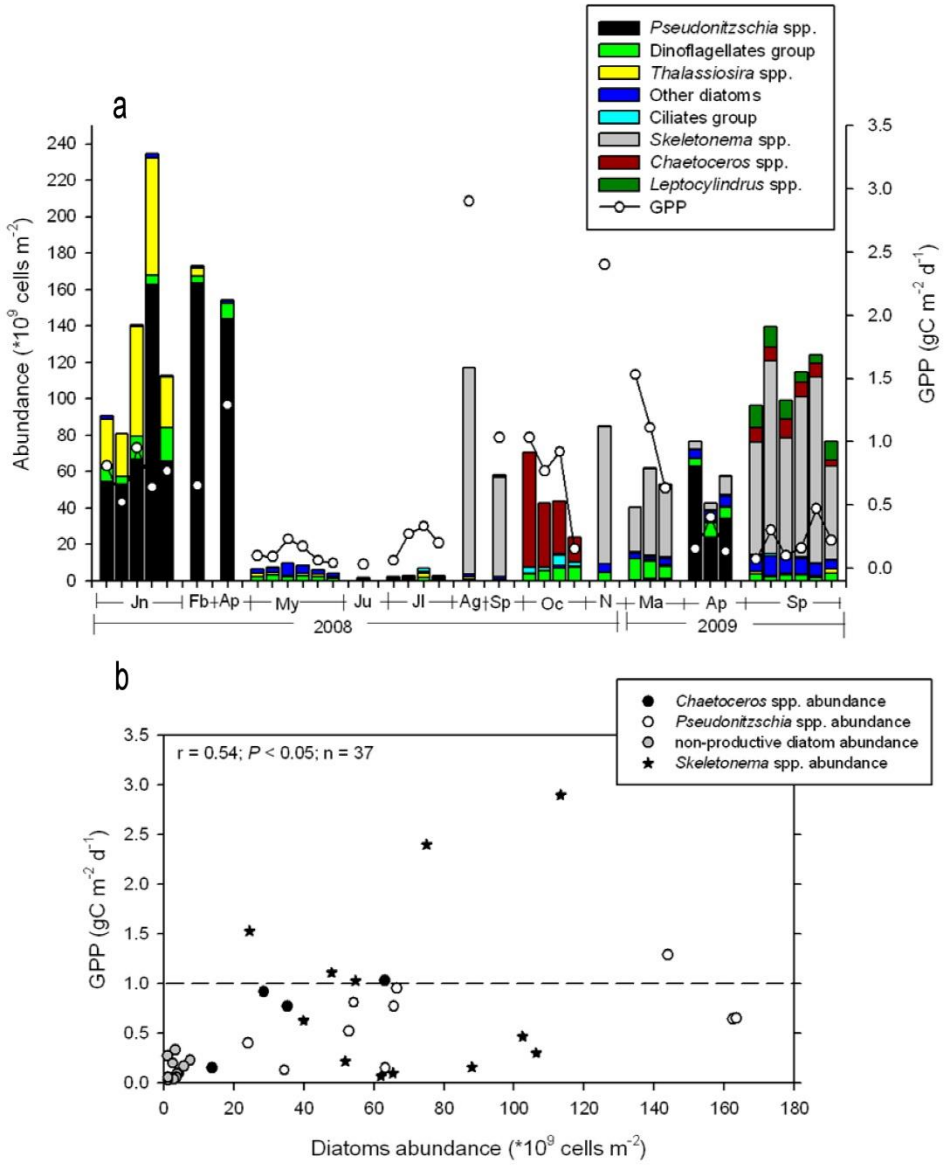


**Figure 8.** Phytoplankton abundance at the Puyuhuapi station. a) Seasonal variability and composition of phytoplankton community, and b) correlation between the dominant diatoms group and GPP values. R value and significance refers to correlation coefficient for all data points.

The dinoflagellate group was composed by *Dinophysis acuminata*, *D. acuta*, *D. rotundatum*, *Heterocapsa triquetra*, *Protoceratium reticulatum*, *Protoperidinium claudicans*, *Protoperidinium* spp., *Gymnodinium* spp., *Ceratium fusus*, *Ceratium lineatum*, *Ceratium* spp., *Prorocentrum micans* and *Alexandrium catenella*. They were present throughout the study period, except *A. catenella* that was only recorded in March 2009. The highest average abundances of this group were observed in January 2008 ($10 \pm 6\times10^9$ cells $m^{-2}$) and March 2009 ($9 \pm 2\times10^9$ cells $m^{-2}$) when sea surface temperature was >13ºC (shown in Fig. 3b). Low abundances were recorded during the non-productive season (0.3 to $3\times10^9$ cells $m^{-2}$).

The ciliate group had highest abundances of between 2 and $6\times10^9$ cells $m^{-2}$ in October 2008 and minimum concentrations (0.2 to $1\times10^9$ cells $m^{-2}$) during the rest of study period.

Seasonal fluctuations in GPP correlated signify-cantly with the abundance of dominant diatoms ($r_s$ = 0.54, n = 37, $P < 0.05$), suggesting that certain key species are mainly associated with high productivity events (Fig. 8b). In fact, the highest levels of GPP (>1.5 g C $m^{-2}$ $d^{-1}$) were recorded when the phytoplankton community was dominated by *Skeletonema* spp. (Fig. 8b).

The highest phytoplankton abundances (23 to $235\times10^9$ cells $m^{-2}$) were generally associated with periods of higher productivity, whereas lowest abundances (2 to $10\times10^9$ cells $m^{-2}$) occurred during the non-productive season. However, a rapid increase in phytoplankton abundance ($117\times10^9$ cell $m^{-2}$) was observed in August 2008 (late winter, non-productive period) suggesting an early onset of spring bloom (Fig. 8a).

The Bray-Curtis cluster analysis (based on the square root transformed phytoplankton abundance) detected four well-defined groups of samples and revealed a seasonal variability (Fig. 9) that coincided with the dominance of certain diatoms during an annual cycle (shown in Fig. 8a). Thus, *Pseudonitzschia* spp. was the dominant group recorded from January-April 2008 and April 2009 (productive season, cluster 1, Fig. 9), "other diatoms" group was from May-July 2008 (non-productive season, cluster 2), *Chaetoceros* spp. dominated the phytoplankton community in October 2008 (productive season, cluster 3) and *Skeletonema* spp. were dominant from August-November 2008, March 2009, and September 2009 (productive season, cluster 4) (Fig. 9).

The principal component analysis (PCA) showed a first (PC1) and second principal component (PC2) that explained 30% and 26.1% of total variance, respect-tively (Fig. 10a). PC1 was positively loaded with salinity and nitrate, while Chl-*a*, silicic acid, *Chaetoceros* spp. and *Skeletonema* spp. were found to be negatively loaded. The second PC was found to be related to a few variables; while salinity and phosphate were positively loaded to PC2, variables such as temperature and *Pseudo-nitzschia* spp. were found to be negatively loaded. The PCA analysis clearly separated three seasonal groups according to different environmental variables: a) a winter group related to salinity, nitrate and orthophosphate, b) a summer-autumn group related to temperature and abundance of *Pseudo-nitzschia* spp. (also dinoflagellates) and c) spring group associated with silicic acid and elevated Chl-*a*, and abundance of *Skeletonema* spp. and *Chaetoceros* spp. (Fig 10b). In this last group March 2009 (Ma09) is an exception because it corresponds to a summer month.

GPP was significantly correlated with PC1 ($r_s$ = -0.6, n = 13, $P < 0.05$) but not with PC2 ($r_s$ = -0.2, n = 13, $P > 0.05$) (Fig. 11).

## DISCUSSION

The analysis of our *in situ* data and longer term records of satellite-derived surface Chl-*a* suggest that the productive season in the northern Puyuhuapi channel begins in late winter (August) and extends until autumn (April). The shorter non-productive season, on the other hand, spans the May-July period, *i.e.*, from late autumn to winter. The transition between these two periods appears to be rather abrupt, although the resolution of our *in situ* observations does not allow us to strongly substantiate this argument. However, similar shifts in other Patagonian fjords have been ascribed to fjord-scale hydrographic changes driven by a seasonal changes in mesoscale wind forcing and solar radiation (Iriarte & González, 2008; Montero *et al.*, 2011; Jacob *et al.*, 2014).

The non-productive season coincides with the seasonal solar radiation minimum, a stronger influence of saltier oceanic waters and a weakening of freshwater driven estuarine circulation, with consequent reduction in water column stratification. Saltier water is driven by predominant westerly winds from the Moraleda Channel into the Puyuhuapi Channel through the Jacaf Channel. In contrast, during the productive season (spring/summer, autumn), estuarine circulation tends to prevail and generates more pronounced water column stratification that is further promoted by increased solar radiation. The freshwater surface layer exits the Puyuhuapi Channel through the Jacaf Channel as water from the Cisnes River is pushed to the north and out towards the Moraleda channel. Overall, the hydrography

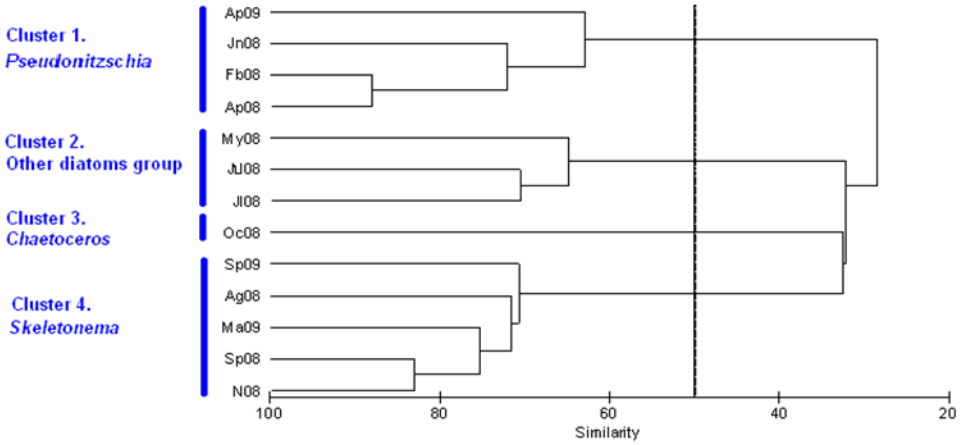


**Figure 9.** Similarity cluster analysis for samples of the phytoplankton community through the whole sampling campaign.

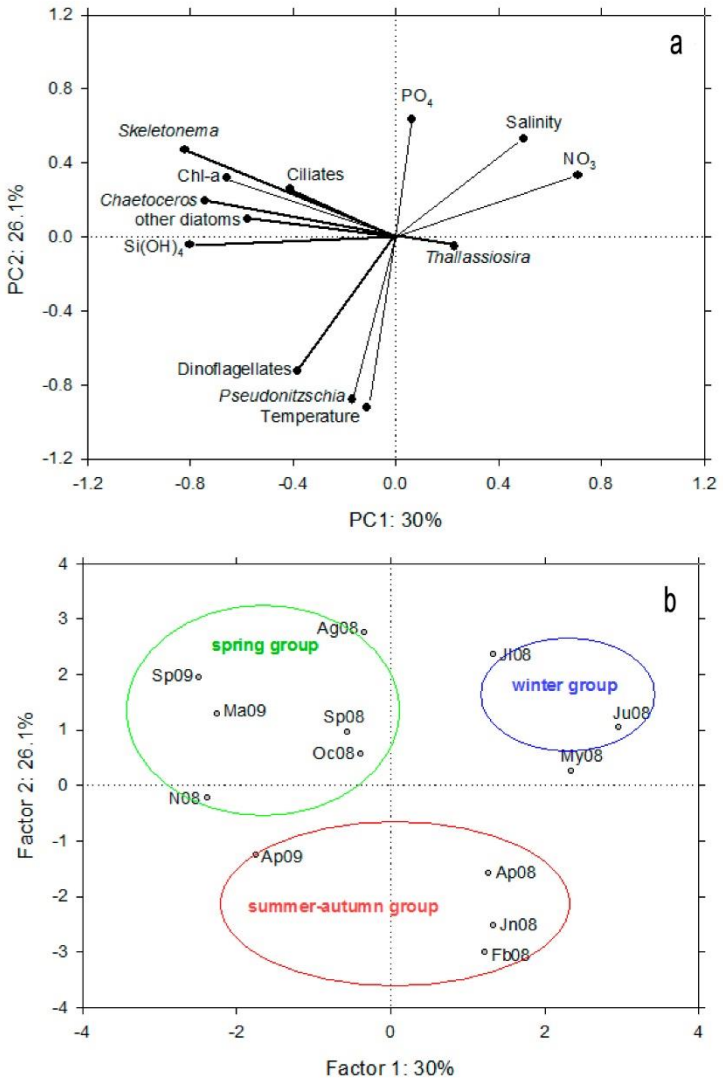


**Figure 10.** Principal component analysis (PCA). a) Ordination diagram of the physical and chemical (temperature, salinity, and inorganic nutrients correspond to depth-averages calculated over the upper 20 m) and biological variables (phytoplankton community and Chl-*a* data corresponded to depth-integrated values calculated down to 20 m), and b) ordination diagram of the sampling month.

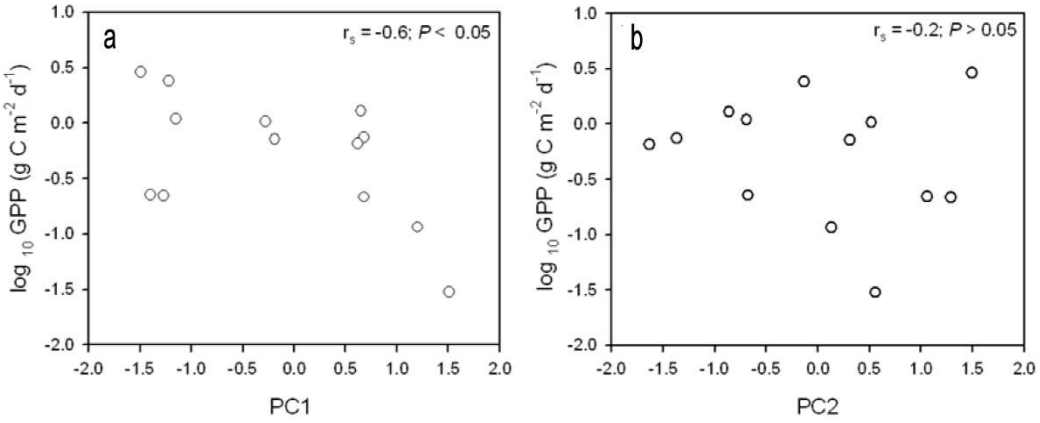


**Figure 11.** a) Significant correlation between gross primary production ($log_{10}$ GPP) and the first principal component, b) non-significant correlation between gross primary production and the second principal component.

of the whole Puyuhuapi channel is strongly influenced by the Cisnes River, which is the main source of freshwater discharge into this basin (Calvete & Sobarzo, 2011; Schneider *et al.*, 2014).

In general, increased freshwater discharge into the channel coincides with increases in the concentrations of silicic acid (20 to 40 µM) and dissolved organic matter concentration, as well as an increase in underwater light attenuation. Periods of intensified freshwater input following a period of reduced flow seem to provide ideal growing conditions for phytoplankton in the Puyuhuapi Channel (G. Daneri, unpublished). However, the time lag in the phyto-plankton's growth response can result in blooms appearing as the freshwater flow recedes. The spring diatom bloom (or late winter bloom in our case) recorded during August 2008 coincided with a ~50% drop in the discharge from the Cisnes River (from 379 $m^3 s^{-1}$ in July to 166 $m^3 s^{-1}$ in August 2008, Fig. 12). In contrast, we recorded reduced phytoplankton activity during periods of increased river freshwater discharge both during the 2008 non-productive period (>200 $m^3 s^{-1}$ between May and July, Fig. 12) and during the 2009 productive period (>200 $m^3 s^{-1}$ between March and September, Fig. 12). Increases in underwater light attenuation associated with increased freshwater input can also explain temporal and spatial variability in phytoplankton production in the fjord areas (Goebel *et al.*, 2005; Jacob *et al.*, 2014; Huovinen *et al.*, 2016).

The range of daily measurements of GPP obtained during the productive season at Puyuhuapi (0.03 to 2.9 g C $m^{-2} d^{-1}$) is in good agreement with high productivity estimates reported by previous studies conducted in other regions of coastal Patagonia, such as the inner sea of Chiloé (41.5º-43ºS; Iriarte *et al.*, 2007), the Reloncaví Fjord (41ºS; Montero *et al.*, 2011), the Aysén region (43º-46ºS; Pizarro *et al.*, 2005) and the Aysén Fjord (45ºS; Lafón *et al.*, submitted). Lowest GPP (0.03 to 0.3 g C $m^{-2} d^{-1}$) and Chl-*a* (2 to 16 mg $m^{-2}$) values were observed during the non-productive season (excluding August). The high variability of integrated GPP values observed during the productive season in Puyuhuapi reflects the pulsed nature and temporal heterogeneity of productivity cycles in the Patagonian fjord region generally. Productivity cycles in similar coastal environments can be modulated by a combination of biological and hydrodynamic controls, both top down (*e.g.*, grazing by predators; González *et al.*, 2011) and bottom-up processes associated to nutrient depletion and replenishment in the photic layer as a consequence of turbulent eddy formation (Farmer & Freeland, 1983), wind stress (Gibbs, 2001), and tidal currents (Cloern, 1982). The annual depth-integrated GPP estimated for the Puyuhuapi study site (329 g C $m^{-2} y^{-1}$) amounts to *ca*. 40% of the yearly GPP estimated for the exceptionally productive upwelling system off Concepción in central Chile (Daneri *et al.*, 2000; Montero *et al.*, 2007), and is of a similar order to estimates in other highly productive fjord ecosystems, such as the Howe sound (~500 g C $m^{-2} y^{-1}$) on the southern coast of British Columbia (Albright & McRae, 1987) and the Gullmar Fjord (~300 g C $m^{-2} y^{-1}$) on the Swedish Skagerrak coast (Lindahl *et al.*, 2009).

Despite these high primary production rates in the Puyuhuapi Channel, and a predominantly autotrophic metabolism in the surface layer (2 m), heterotrophic activity throughout the water column was also significant throughout the year, probably sustained by the input of allochthonous organic matter of terrestrial origin together with organic material derived from salmon cage farming; these sources would allow to use more organic carbon than that produced within the system (Montero *et al.*, 2011).

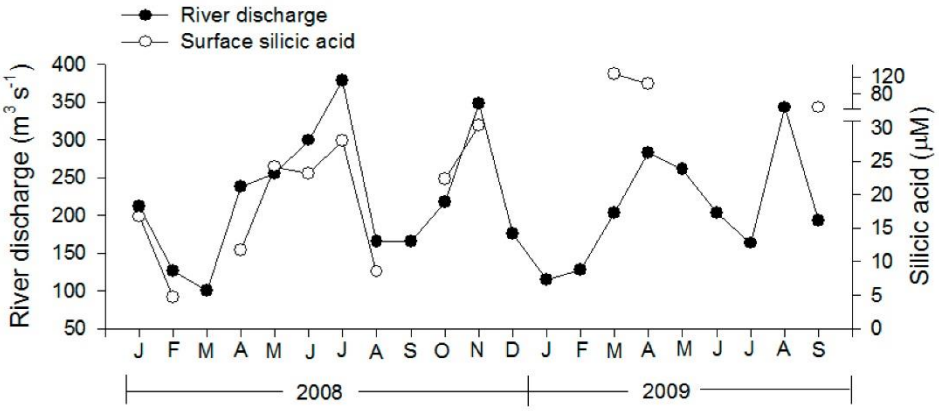


**Figure 12.** Cisnes River discharge and its association with the silicic acid measurements in surface water, at the Puyuhuapi station.

The phase change between productive and non-productive seasons in Puyuhuapi Channel was reflected in changes in relative abundance of the three-phytoplankton size fractions. Large phytoplankton (>20 µm; mainly diatoms) dominated total abundance and showed the highest contribution to total carbon fixation during the productive season. In contrast, the small picophytoplankton size fraction (<2 µm) was dominant during non-productive season when they made their maximum contributions to primary production rates. These results support the notion that diatoms tend to dominate in the productive season, while small photosynthetic cells become more important under harsher environmental conditions.

In our study, diatoms of the genera *Skeletonema*, *Chaetoceros* and *Pseudo-nitzschia* dominated and showed a marked seasonality that was reflected in the Bray-Curtis analysis. *Skeletonema* spp. generally dominated between the beginning of the productive season in late winter (August) and spring, while *Chaetoceros* spp. and *Pseudo-nitzschia* spp. dominated the spring and summer-autumn seasons, respectively. The PCA analysis suggested that this marked seasonality is driven by environmental conditions and suggested that warm waters were associated with high concentrations of *Pseudo-nitzschia* spp., whereas elevated abundances of *Skeletonema* spp. and *Chaetoceros* spp. were associated with silicate-rich waters. Our data are consistent with other studies in the southern fjord system of Patagonia, where the phytoplankton community shows recurring changes in dominance and diversity of a number of diatom species (Iriarte *et al.*, 2007; Alves-de-Souza *et al.*, 2008; Iriarte and González, 2008; Montero *et al.*, 2011), some of which have also been recorded in the sediments of the Puyuhuapi Channel (Rebolledo *et al.*, 2005).

The almost complete absence of coexisting species observed during the blooms of *Skeletonema* spp. in August, September and November 2008, and *Pseudo-nitzschia* spp. in February and April 2008 is indicative of a strong competitive ability of these genera. In a highly mixed and disturbed environment, enhanced competitive ability for resources is probably the main factor favouring the dominance of certain species. However it is interesting to note that field and laboratory experiments have shown that *Skeletonema* and *Pseudo-nitzschia* species can release allelophatic compounds (*e.g.*, Lundholm *et al*., 2005*;* Yamasaki *et al*., 2010; Xu *et al*., 2015) that could also be a factor in promoting mono-specific blooms in the channel.

We observed an inverse association between diatoms and concentrations of nitrate and orthophosphate, reflecting the depletion of these nutrients from the water column by this dominant group. Despite the marked drawdown in concentrations during the productive season, nutrients tend not be depleted below the known half saturation constant of several diatoms, (*e.g.*, Eppley *et al.*, 1969); and this likely results from periodic entrainment processes that replenish these nutrients. The resulting continuous availability of nutrients is probably the major factor behind the exceptionally long productive season (from late winter to late autumn), observed for the Puyuhuapi Channel (this study) and Reloncaví Fjord (Montero *et al.*, 2011). The vertical separation in the sources of silicic acid from surface freshwater, and nitrate and phosphate from deeper oceanic water is an interesting feature of these fjord systems (Torres *et al.*, 2014). Because of this, nitrate and phosphate are replenished by entrainment of oceanic water, whereas the levels of silicic acid in Patagonian fjords are enhanced by river input which results in higher than normal ratios for $Si[OH]_4:NO_3$ (5) and $Si[OH]_4:PO_4$ (36). Thus, the observed dominance of diatoms in the phytoplankton

community of the study area was likely facilitated by a high concentration and relatively constant supply of silicic acid. The $NO_3$:$PO_4$ ratio (~9) also shows a deviation from Redfield, confirming the preferential assimilation of nitrogen in Chilean fjords (Iriarte *et al.*, 2007, 2013).

Maximum abundance of phytoplankton was observed when *Pseudo-nitzschia* spp. dominated (February to April 2008; 140 to $164\times10^9$ cells $m^{-2}$) but the highest GPP rates were associated with the presence of *Skeletonema* spp. during late winter (August; $113\times10^9$ cells $m^{-2}$) and spring (November; $75\times10^9$ cells $m^{-2}$). The high GPP, but lower abundance conditions associated with *Skeletonema* blooms may be the result of elevated photosynthetic rates shown by species of this genus (Han *et al.*, 1992; Liu *et al.*, 2005; Li *et al.*, 2009) and top-down controls (*e.g.*, grazing) being exerted on this species by zooplankton populations that peak in the area at the beginning of the productive season (González *et al.*, 2011).

GPP rates were significantly correlated with the first principal component, where high GPP values were more associated with negative (high silicic acid concentration, high Chl-*a*, and increase in abundance of *Skeletonema* and *Chaetoceros*) than positive values of PC1 (high nitrate concentration and high salinity). This suggests that the flow of freshwater (with high silicic acid concentration) into the channel could therefore be a key factor in regulating the onset of productive periods, and indeed in the overall annual productivity in Puyuhuapi Channel. Rebolledo *et al.* (2005) have noted a decrease in the contribution of freshwater diatoms to sediments of Puyuhuapi Channel since the 1970s, which they attributed to a decline in rainfall in the area associated with climate change. A variety of productivity proxies in sediments also suggest that periods of low rainfall have coincided with decreased overall productivity within the Puyuhuapi channel (Sepúlveda *et al.*, 2005). Over the whole system of Patagonian Fjords, the silicic acid to $NO_3$ deficit increases in a southerly direction, with the consequence of more frequent non-diatom blooms to the south (Torres *et al.*, 2014).

We therefore suggest that under a scenario of climate change characterized by reduced freshwater input into Patagonian Fjords such as Puyuhuapi Channel, the reduced supply of silicic acid may consequently alter the composition of phytoplankton community towards an increased proportion of dinoflagellates and/or other non-silicified species (Olsen *et al.*, 2014), and potentially change the biological productivity in the region. Low silicic acid concentrations could specifically also limit the presence of certain productive species in the water column such as *Skeletonema costatum*, which in addition to being associated with high levels of silicate in Patagonian fjords (Alves de Souza *et al.*, 2008; Labbé-Ibañez *et al.*, 2015), has been in this and other studies (Montero *et al.*, 2011) correlated significantly with high rates of primary production (GPP). Accordingly, the impact would not only be on community composition, but also on carbon export fluxes, and on the supply and transfer of food/organic matter to higher trophic levels in these unique coastal ecosystems.

## ACKNOWLEDGEMENTS

This research was funded by FONDECYT 1070713 and (partially) COPAS Sur-Austral Program (CONICYT PFB-31) (G. Daneri and P. Montero). Funding for FT and JLI was provided by the COPAS Sur-Austral Program (CONICYT PFB-31).

## REFERENCES

Albright, L.J. & S.K. McCrae. 1987. Annual bacterioplankton biomasses and productivities in a temperate west coast Canadian fjord. Appl. Environ. Microbiol., 53(6): 1277-1285.

Amin, S.A., M.S. Parker & E.V. Armbrust. 2012. Microbiol. Mol. Biol. R., 76(3): 667-684.

Alves-de-Souza, C., M.T. González & J.L. Iriarte. 2008. Functional groups in marine phytoplankton assemblages dominated by diatoms in fjords of southern Chile. J. Plankton Res., 30: 1233-1243.

Bray, J.R. & J.T. Curtis. 1957. An ordination of upland forest community of Southern Wisconsin. Ecol. Monogr., 27: 325-349.

Calvete, C. & M. Sobarzo. 2011. Quantification of the surface brackish water layer and frontal zones in southern Chilean fjords between Boca del Guafo (43º30'S) and Estero Elefantes (46º30'S). Cont. Shelf Res., 31(3-4): 162-171.

Cassis, D., P. Muñoz & S. Avaria. 2002. Variación temporal del fitoplancton entre 1993 y 1998 en una estación fija del Seno Aysén, Chile (45º26'S-73º00'W). Rev. Biol. Mar. Oceanogr., 37(1): 43-65.

Chaigneau, A. & O. Pizarro, 2005. Mean surface circulation and mesoscale turbulent flow characteristics in the eastern South Pacific from satellite tracked drifters. J. Geophys. Res., 110, C05014, doi: 10.1029/2004JC002628.

Cloern, J.E. 1982. Does the benthos control phytoplankton biomass in south San Francisco Bay? Mar Ecol. Prog. Ser., 9: 191-202.

Czypionka, T., C.A. Vargas, N. Silva, G. Daneri, H.E. González & J.L. Iriarte. 2011. Importance of mixotrophic nanoplankton in Aysén Fjord (Southern Chile) during austral winter. Cont. Shelf Res., 31(3-4): 216-224.

Daneri, G., V. Dellarossa, R. Quiñones, B. Jacob, P. Montero & O. Ulloa. 2000. Primary production and community respiration in the Humboldt Current System off Chile and associated oceanic areas. Mar. Ecol. Prog. Ser., 197: 41-49.

Eppley, R.W., J.N. Rogers & J.J. McCarthy. 1969. Half-saturation constants for uptake of nitrate and ammonium by marine phytoplankton. Limnol. Oceanogr., 14: 912-920.

Farmer, D.M. & H.J. Freeland. 1983. The physical oceanography of fjords. Prog. Oceanogr., 12: 147-220.

Ferland, J., M. Gosselin & M. Starr. 2011. Environmental control of summer primary production in the Hudson Bay system: the role of stratification. J. Mar. Syst., 88: 385-400.

Gibbs, M.T. 2001. Aspects of the structure and variability of the low-salinity-layer in Doubtful Sound, a New Zealand fjord. New Zeal. J. Mar Freshw. Res., 35: 59-72.

Goebel, N.L., S.R. Wing & P.W. Boyd. 2005. A mechanism for onset of diatom blooms in a fjord with persistent salinity stratification. Estuar. Coast. Shelf. Sci., 64: 546-560.

González, H.E., M.J. Calderon, L. Castro, A. Clement, L.A. Cuevas, G. Daneri, J.L. Iriarte, L. Lizárraga, R. Martínez, E. Menschel, N. Silva, C. Carrasco, C. Valenzuela, C.A. Vargas & C. Molinet. 2010. Primary Production and plankton dynamics in the Reloncaví Fjord and the Interior Sea of Chiloé, Northern Patagonia, Chile. Mar. Ecol. Prog. Ser., 402: 13-30.

González, H.E., L. Castro, G. Daneri, J.L. Iriarte, N. Silva, C.A. Vargas, R. Giesecke & N. Sánchez. 2011. Seasonal plankton variability in Chilean Patagonia fjords: carbon flow through the pelagic food web of Aysén Fjord and plankton dynamics in the Moraleda Channel basin. Cont. Shelf Res., 31: 225-243.

González, H.E., L.R. Castro, G. Daneri, J.L. Iriarte, N. Silva, F. Tapia, E. Teca & C.A. Vargas. 2013. Land-ocean gradient in haline stratification and its effects on plankton dynamics and trophic carbon fluxes in Chilean Patagonian fjords (47-50ºS). Prog. Oceanogr., 119: 32-47.

Huovinen, P., J. Ramírez & I. Gómez. 2016. Underwater optics in sub-Antarctic and Antarctic coastal ecosystems. PLoS ONE, 11(5): e0154887. doi:10. 1371/journal.pone.0154887.

Iriarte, J.L., A. Kusch, J. Osses & M. Ruiz. 2001. Phytoplankton biomass in the sub-Antarctic area of the Straits of Magellan (53ºS), Chile during spring-summer 1997/1998. Polar Biol., 24: 154-162.

Iriarte, J.L., H.E. González, K.K. Liu, C. Rivas & C. Valenzuela. 2007. Spatial and temporal variability of chlorophyll and primary productivity in surface waters of southern Chile (41.5-43ºS). Estuar. Coast. Shelf Sci., 74: 471-480.

Iriarte, J.L. & H.E. Gonzalez. 2008. Phytoplankton bloom ecology of the inner Sea of Chiloé, Southern Chile. Nova Hedwigia, Beiheft, 133: 67-79.

Iriarte, J.L., S. Pantoja, H.E. González, G. Silva, H. Paves, P. Labbé, L. Rebolledo, M. Van Ardelan & V. Häussermann. 2013. Assessing the micro-phytoplankton response to nitrate in Comau Fjord (42ºS) in Patagonia (Chile), using a microcosms approach. Environ. Monit. Assess., 185: 5055-5070.

Iriarte, J.L., S. Pantoja & G. Daneri. 2014. Oceanographic processes in Chilean fjords of Patagonia: from small to large-scale studies. Prog. Oceanogr., 129: 1-7.

Jacob, B.G., F. Tapia, G. Daneri, J.L. Iriarte, P. Montero, M. Sobarzo & R.A. Quiñones. 2014. Springtime size-fractionated primary production across hydrographic and PAR-light gradients in Chilean Patagonia (41-50ºS). Progr. Oceanogr., 129: 75-84.

Lafón, A., P. Montero, G. Daneri, J.L. Iriarte, V. San Martín, M. Araya & C.A. Vargas. Allochthonous organic carbon sources and primary production in the Aysén Fjord, northern Patagonia. (submitted).

Legrand, C., K. Rengefors, G.O. Fistarol & E. Granéli. 2003. Allelopathy in phytoplankton - biochemical, ecological and evolutionary aspects. Phycologia, 42(4): 406-419.

Li, C., B. Zhu, H. Chen, Z. Liu, B. Cui, J. Wu, B. Li, H. Yu & M. Peng. 2009. The relationship between the *Skeletonema costatum* red tide and environmental factors in Hongsha Bay of Sanya, South China Sea. J. Coastal Res., 25(3): 651-658.

Lindahl, O., L. Andersson & A. Belgrano. 2009. Primary phytoplankton productivity in the Gullmar Fjord, Sweden: an evaluation of the 1985-2008 time series. Swed. Environ. Protec. Agency Rep., 6309, 35 pp.

Liu, D., J. Sun, J. Zou & J. Zhang. 2005. Phytoplankton succession during a red tide of *Skeletonema costatum* in Jiaozhou Bay of China. Mar. Pollut. Bull,. 50: 91-94.

Lundholm, N., P.J. Hansen & Y. Kotaki. 2005. Lack of allelopathic effects of the domoic acid-producing marine diatom *Pseudo-nitzschia multiseries*. Mar. Ecol. Prog. Ser., 288: 21-33.

Montecino, V., M.A. Paredes, P. Paolini & J. Rutllant. 2006. Revisiting chlorophyll data along the coast in north-central Chile, considering multiscale environmental variability. Rev. Chil. Hist. Nat., 79: 213-223.

Montero, P., G. Daneri, L.A. Cuevas, H.E. González, B. Jacob, L. Lizárraga & E. Menschel. 2007. Productivity cycles in the coastal upwelling area of Concepción: the importance of diatoms and bacterioplankton in the organic carbon flux. Prog. Oceanogr., 75(3): 518-530.

Montero, P., G. Daneri, H.E. González, J.L. Iriarte, F.J. Tapia, L. Lizárraga, N. Sanchez & O. Pizarro. 2011. Seasonal variability of primary production in a fjord ecosystem of the Chilean Patagonia: implications for the transfer of carbon within pelagic food webs. Cont. Shelf Res., 31: 202-215.

Olsen, L.M., K.L. Hernández, M. Van Anderlan, J.L. Iriarte, N. Sánchez, H.E. González, N. Tokle & Y. Olsen. 2014. Responses in the microbial food web to increased rates of nutrient supply in a southern Chilean fjord: possible implications of cage aquaculture. Aquacult. Environ. Interact., 6: 11-27.

Parsons, T.R., Y. Maita & C.M. Lalli. 1984. Counting, media and preservatives. In: T.R. Parsons, Y. Maita & C.M. Lalli (eds.). A manual of chemical and biological methods for seawater analysis. Pergamon Press, Oxford, 173 pp.

Paredes, M.A. & V. Montecino. 2011. Size diversity as an expression of phytoplankton community structure and the identification of its patterns on the scale off fjords and channels. Cont. Shelf Res., 31: 272-281.

Pizarro, G., R. Astoreca, V. Montecino, M.A. Paredes, G. Alarcón, P. Uribe & L. Guzmán. 2005. Patrones espaciales de la abundancia de la clorofila, su relación con la productividad primaria y la estructura de tamaños del fitoplancton en Julio y Noviembre de 2001 en la región de Aysén (43°-46°S). Rev. Cienc. Tecnol. Mar, 28(2): 27-42.

Poole, H.H. & W.R.G. Atkins. 1929. Photo-electric measurements of submarine illumination throughout the year. J. Mar. Biol. Assoc. UK, 16: 297-324.

Rebolledo, L., C.B. Lange, D. Figueroa, S. Pantoja, P. Muñoz & R. Castro. 2005. 20$^{th}$ century fluctuations in the abundance of siliceous microorganisms preserved in the sediments of the Puyuhuapi Channel (44°S), Chile. Rev. Chil. Hist. Nat., 78: 469-488.

Sarthou, G., K.R. Timmermans, S. Blain & P. Tréguer. 2005. Growth physiology and fate of diatoms in the ocean: a review. J. Sea Res., 53: 25-42.

Schneider, W., I. Pérez-Santos, L. Ross, L. Bravo, R. Seguel & F. Hernández. 2014. On the hydrography of Puyuhuapi Channel (Chilean Patagonia). Prog. Oceanogr., 129: 8-18.

Sciremammano, F. 1979. A suggestion for the presentation of correlations and their significance levels. J. Phys. Oceanogr., 9: 1273-1276.

*Received: 30 December 2016; Accepted: 5 July 2017*

Sepúlveda, J., S. Pantoja, K. Hughen C. Lange, F. Gonzalez, P. Muñoz, L. Rebolledo, R. Castro, S. Contreras, A. Ávila, P. Rossel, G. Lorca, M. Salamanca & N. Silva, 2005. Fluctuations in export productivity over the last century from sediments of a southern Chilean fjord (44ºS). Estuar. Coast. Shelf Sci., 65: 587-600.

Silva, N. 2008. Dissolved oxygen, pH, and nutrients in the austral Chilean channels and fjords. Progress in the oceanographic knowledge of Chilean interior waters, from Puerto Montt to Cape Horn. In: N. Silva & S. Palma (eds.). Comité Oceanográfico Nacional-Pontificia Universidad Católica de Valparaíso, Valparaíso, pp. 37-43.

Silva, N., N. Rojas & N. Fedele. 2009. Water masses in the Humboldt Current System: properties, distribution and the nitrate deficit as a chemical water mass tracer for Equatorial Subsurface Water off Chile. Deep-Sea Res. II, 56: 1004-1020.

Steeman-Nielsen, E. 1952. The use of radioactive carbon ($C^{14}$) for measuring organic production in the sea. J. Cons. Perm. Int. Explor. Mer, 18(2): 117-140.

Strickland, J.D.H. 1960. Measuring the production of marine phytoplankton. Bull. Fish Res. Bd. Can., 122: 1-172.

Strickland, J.D.H. & T.R. Parsons. 1968. A practical handbook of seawater analysis. Bull. Fish. Res. Bd. Can., 167 pp.

Torres, R., N. Silva, B. Reid & M. Frangopulos. 2014. Silicic acid enrichment of Subantarctic Surface Water from continental inputs along the Patagonian archipelago interior sea (41-56ºS). Prog. Oceanogr., 129: 50-61.

Utermöhl, H. 1958. Zur Vervollkommnung der quantitativen Phytoplankton-Methodik. Internationale Vereinigung für Theoretische und Angewandte Limnologie. Komitee für Limnologische Methoden, 9: 1-39.

Wetz, M.S. & P.A. Wheeler. 2007. Release of dissolved organic matter by coastal diatoms. Limnol. Oceanogr., 52(2): 798-807.

Williams, P.J.LeB. & J.E. Robertson. 1991. Overall planktonic oxygen and carbon dioxide metabolism: the problem of reconciling observations and calculations of photosynthetic quotients. J. Plankton Res., 13: 153-169.

Xu, N., Y.Z. Tang, S. Duan & C.J. Gobler. 2015. Ability of the marine diatoms *Pseudo-nitzschia multiseries* and *P. pungens* to inhibit the growth of co-occurring phytoplankton via allelopathy. Aquat. Microbiol. Ecol., 74: 29-41.

Yamazaki, Y., Y. Ohmichi, T. Shikata, M. Hirose, Y. Shimasaki, Y. Oshima & T. Honjo. 2010. Species-specific allelopathic effects of the diatom *Skeletonema costatum*. Thalassas, 27(1): 21-32.